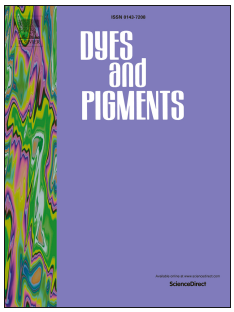

Synthesis and luminescence properties of analogues of the green fluorescent protein chromophore

Cátia I.C. Esteves, Inês da Silva Fonseca, João Rocha, ArturM.S. Silva, Samuel Guieu

PII: S0143-7208(19)32582-3

DOI: https://doi.org/10.1016/j.dyepig.2020.108267

Reference: DYPI 108267

To appear in: *Dyes and Pigments*

Received Date: 5 November 2019

Revised Date: 6 February 2020

Accepted Date: 6 February 2020

Please cite this article as: Esteves CáIC, da Silva Fonseca Inê, Rocha Joã, Silva AS, Guieu S, Synthesis and luminescence properties of analogues of the green fluorescent protein chromophore, *Dyes and Pigments* (2020), doi: https://doi.org/10.1016/j.dyepig.2020.108267.

Cátia I. C. Esteves: Investigation, Visualization, Writing – original draft,

Inês da Silva Fonseca: Investigation, Visualization,

João Rocha: Funding acquisition, Writing – review & editing,

Artur M. S. Silva: Funding acquisition, Writing – review & editing,

Samuel Guieu: Conceptualization, Funding acquisition, Project administration, Supervision, Writing – original draft, Writing – review & editing,

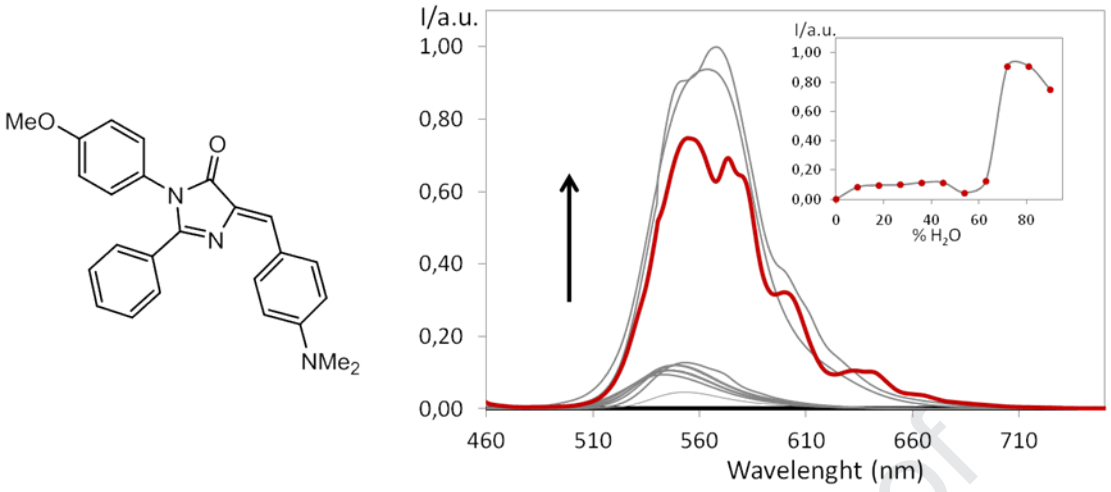

Synthesis and Luminescence Properties of Analogues of the Green Fluorescent Protein Chromophore

Cátia I. C. Esteves,[a] Inês da Silva Fonseca,[a] João Rocha,[b] Artur M. S. Silva,[a] Samuel Guieu[a,b,*]

[a] LAQV/REQUIMTE, QOPNA, Department of Chemistry, University of Aveiro, 3810-193 Aveiro, Portugal.
[b] CICECO-Aveiro Institute of Materials, Department of Chemistry, University of Aveiro, 3810-193 Aveiro, Portugal.

E-mail: sguieu@ua.pt ; rocha@ua.pt ; artur.silva@ua.pt ; catiaiesteves@ua.pt

Abstract

The green fluorescent protein (GFP) is extensively used as a biomarker for fluorescence biological imaging. The chromophore in GFP is only fluorescent when confined into the β–barrel of the protein. Similarly, synthetic analogues of the fluorophore of GFP are usually non-emissive in solution, due to free rotation around the aryl-alkene bond and (*Z*/*E*)-isomerization of the double bond. Here, the synthesis and characterization of three analogues of the fluorophore of GFP are reported. The introduction of more electron donating substituents induces a red-shift in the absorption and emission. The fluorophores are more emissive in the solid state than in solution, and a study of their crystal structure reveals that the (*Z*/*E*)-isomerization is efficiently blocked in the crystals.

Key words
Green fluorescent protein; Aggregation-Induced Emission Enhancement; Synthesis; fluorescence

1. Introduction

The green fluorescent protein (GFP) from the jellyfish *Aequorea victoria* is extensively used as a biomarker for fluorescence biological imaging [1]. Fusion of GFP with other proteins allows their visualization in living cells, usually without affecting their function [2]. GFP is therefore used in molecular and cell biology, in cell-labeling and bioimaging applications, as genetically encoded fluorescent marker in biology, in live cell imaging and in medicine [3]. Other fluorescent proteins emit light with different colors, but all have a similar cylindrical structure, with the chromophore enclosed in a central α-helix. In the wild type GFP, the chromophore responsible for the fluorescence is the *p*-hydroxybenzylideneimidazolidinone (Figure 1), which emits through excited-state proton transfer from the phenolic oxygen to the protein β-barrel [4]. An interesting point is that the chromophore is non-emissive when it is isolated from the protein ($\Phi < 10^{-3}$), due to a non-radiative relaxation channel through the

(*Z*/*E*)-isomerization of the benzylidene substituent. The chemical environment ensuring the autocatalytic formation of the chromophore from three amino acids is also responsible for the rigidly defined and firmly packed structure of the protein [5]. The fluorescent proteins efficiently block the (*Z*/*E*)-isomerisation of the fluorophore, turning it emissive (Φ = 0.8) [6].

Synthetic analogues of the GFP chromophore have been prepared [2] and applied to biological imaging, with some success [4,5]. The synthesis usually starts with the condensation of a hippuric acid derivative with an aldehyde, the so called "Erlenmeyer azlactone synthesis", followed by further modifications [4,8]. Various strategies have been developed in order to turn the analogues emissive in dilute solutions, such as rigidification of the backbone through chemical modification [8b] or introduction of boron complex [9]. Nevertheless, the fluorophores are always more emissive when their motion is restraint than they are when in dilute solutions, and crystallization or precipitation are efficient ways of restricting the molecular motion in small organic molecules.
Some analogues of the GFP fluorophore show Aggregation-Induced Emission Enhancement (AIEE) properties [10]. Following previous works on AIEE [11], we have now designed fluorophores with aromatic groups rotating around the imidazolidinone core, in order to increase the AIEE effect.

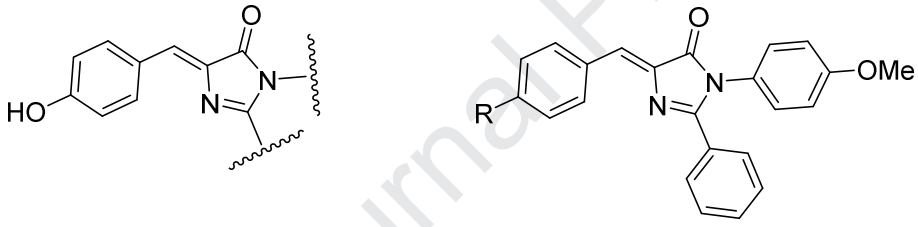

Figure 1. Structure of the GFP chromophore and analogues.

2. Experimental

Melting points were measured with a Büchi Melting Point B-540 apparatus and are uncorrected. NMR spectra were recorded on a Bruker DRX Avance 300 spectrometer (300.13 MHz for ^{1}H, 75.47 MHz for ^{13}C), in $CDCl_3$ or DMSO-d_6 as solvents, if not stated otherwise. Chemical shifts (δ) are reported in ppm from TMS and coupling constants (*J*) in Hz; internal standard was residual peak of the solvent. Unequivocal ^{13}C assignments were made with the aid of 2D *g*HSQC and *g*HMBC (delays for one-bond and long-range *J* C/H couplings were optimised for 145 and 7 Hz, respectively) experiments. Positive-ion ESI mass spectra were acquired using a Q-TOF 2 instrument [Nitrogen was used as nebuliser gas and argon as collision gas. The needle voltage was set at 3000 V, with the ion source at 80°C and desolvation temperature at 150°C. Cone voltage was 35 V]. Preparative thin-layer chromatography was performed with Merck silica gel (60 DGF_{254}). Column chromatography

was performed with Merck silica gel 60 (70−230 mesh). All other chemicals and solvents used were obtained from commercial sources and were either used as received or dried by standard procedures.

*2.1. General procedure for the synthesis of Oxazolone derivatives **2a-c***

Hippuric acid (5 mmol), sodium acetate (5 mmol), benzaldehyde derivative (5 mmol) and acetic anhydride (40 mmol) were stirred at 100 ºC for 1-24 h. The reaction was allowed to cool down to room temperature. It was poured onto ice (50 g) and H_2O (100 mL) and the precipitate that formed was collected by filtration. Then, the obtained solid was dissolved in CH_2Cl_2 and dried over anhydrous Na_2SO_4. The solvent was evaporated to dryness and the obtained residues were recrystallized from EtOH. Compounds **2a-c** have already been described in the literature [20].

*2.1.1 (Z)-4-[4-(dimethylamino)benzylidene]-2-phenyl-1,3-oxazol-5(4H)-one (**2a)*** [20]

The product was isolated as a red solid (0.598 g, 2.0 mmol, 41 %). M.p. = 218-219 ºC. ^{1}H NMR (300 MHz, $CDCl_3$) δ = 3.10 (s, 6H, $N(CH_3)_2$), 6.74 (d, *J* = 9.3 Hz, 2H, H-3',5'), 7.20 (s, 1H, CH), 7.50-7.54 (m, 3H, H-3'', H-4'' and H-5''), 8.12-8.16 (m, 4H, H-2',6' and H-2'',6'') ppm.

*2.1.2 (Z)-4-(4-methoxybenzylidene-2-phenyl-1,3-oxazol-5(4H)-one (**2b)***

The product was isolated as a yellow solid (0.654 g, 2.3 mmol, 47 %). M.p. = 157-158 ºC. ^{1}H NMR (300 MHz, $CDCl_3$) δ = 3.89 (s, 3H, OCH_3), 7.00 (dd, *J* = 9.0 and 2.4 Hz, 2H, H-3',5'), 7.22 (s, 1H, CH), 7.52-7.60 (m, 3H, H-3'', H-4'' and H-5''), 8.15-8.21 (m, 4H, H-2',6' and H-2'',6'') ppm.

*2.1.3 (Z)-4-(4-nitrobenzylidene-2-phenyl-1,3-oxazol-5(4H)-one (**2c)***

The product was isolated as a yellow solid (0.496 g, 1.7 mmol, 34%). M.p. = 239-240 ºC. ^{1}H NMR (300 MHz, $CDCl_3$) δ = 7.24 (s, 1H, CH), 7.56-7.61 (m, 2H, H-3'',5''), 7.66-7.71 (m, 1H, H-4''), 8.21-8.24 (m, 2H, H-2'',6''), 8.31-8.40 (m, 4H, H-2',6' and H-3',5') ppm.

*2.2. General procedure for the synthesis of Benzamide derivatives **3a-c***

Oxazolone derivatives (1 mmol) and *p*-anisidine (1.5 mmol) were stirred solvent free at ~70ºC for 4-24 h. Then, the solid was taken up in CH_2Cl_2 (30 mL) and dried over anhydrous Na_2SO_4. The solvent was evaporated to dryness and the obtained residues were recrystallized from ethyl acetate.

*2.2.1. (E)-N-(1-(4-(dimethylamino)phenyl)-3-((4-methoxyphenyl)amino)-3-oxoprop-1-en-2-yl)benzamide (**3a**)* [20]

The product was isolated as a yellow solid (0.330 g, 0.79 mmol, 79 %). M.p. = 243-244 ºC. ^{1}H NMR (300 MHz, DMSO-d_6) δ = 2.93 (s, 6H, $N(CH_3)_2$), 3.74 (s, 3H, OCH_3), 6.69 (d, *J* 9.0 Hz, 2H, H-3',5'), 6.89 (d, *J* = 9.0 Hz, 2H, H-3'',5''), 7.19 (s, 1H, CH), 7.49-7.63 (m, 7H, H-2',6', H-2'',6'', H-3''', 5''' and H-4'''), 8.07 (d, *J* = 6.9 Hz, 2H, H-2''',6'''), 9.79 (s, 1H, NH), 9.90 (s, 1H, NH) ppm. ^{13}C NMR (75 MHz, DMSO-d_6) δ = 41.0 ($N(CH_3)_2$), 55.1 (OCH_3), 111.6 (C-3',5'), 113.6 (C-3'',5''), 121.5 (C-1'), 121.7 (C-2'',6''), 125.9 (NH*C*CO), 127.9 (C-2''',6'''), 128.3 (C-3''',5'''), 130.2 (CH), 131.1 (C-3',5'), 131.6 (C-4'''), 132.6 (C-

1’’), 133.9 (C-1’’’), 150.5 (C-4’), 155.1 (C-4’’), 164.1 (C*C*ONH), 165.9 (*C*ONHC) ppm. MS *m/z* (ESI %): 416.2 ($[M+H]^+$); HMRS: m/z (ESI) calc. for $C_{25}H_{26}N_3O_3$ 416.1969, found 416.1990.

*2.2.2. (E)-N-(1-(4-methoxyphenyl)-3-((4-methoxyphenyl)amino)-3-oxoprop-1-en-2-yl)benzamide (**3b**)*

The product was isolated as a white solid (0.319 g, 0.79 mmol, 73 %). M.p. = 233-235 ºC. ^{1}H NMR (300 MHz, DMSO-d_6) δ = 3.74 (d, *J* = 1.8 Hz, 3H, OCH_3), 3.77 (d, *J* = 1.6 Hz, 3H, OCH_3), 6.90 (dd, *J* = 8.9 and 1.8 Hz, 2H, H-3’’,5’’), 6.96 (dd, *J* = 8.4 and 1.6 Hz, 2H, H-3’,5’), 7.17 (s, 1H, CH), 7.51-7.64 (m, 7H, H-2’,6’, H-2’’,6’’, H-3’’’,5’’’ and H-4’’’), 8.05 (d, *J* = 8.1 Hz, 2H, H-2’’’,6’’’), 9.94 (s, 1H, NH), 10.00 (s, 1H, NH) ppm. ^{13}C NMR (75 MHz, DMSO-d_6) δ = 55.1 (OCH_3), 55.2 (OCH_3), 113.6 (C-3’’,5’’), 114.0 (C-3’,5’), 121.7 (C-2’’,6’’), 126.7 (C-1’), 127.9 (C-2’’’,6’’’), 128.3(C-2’,6’), 128.5 (CH), 128.8 (C-4’’’), 131.1 (C-3’’’,5’’’), 131.7 (NH*C*CO), 132.4 (C-1’’), 133.6 (C-1’’’), 155.3(C-4’’), 159.5 (C-4’), 164.1 (C*C*ONH), 165.9 (*C*ONHC) ppm. MS *m/z* (ESI %): 403.2 ($[M+H]^+$); HMRS: m/z (ESI) calc. for $C_{24}H_{23}N_2O_4$ 403.1652, found 403.1669.

*2.2.3. (E)-N-(1-(4-nitroxyphenyl)-3-((4-methoxyphenyl)amino)-3-oxoprop-1-en-2-yl)benzamide (**3c**)*

The product was isolated as a white solid (0.143 g, 0.34 mmol, 50%). M.p. = 232-233 ºC. ^{1}H NMR (300 MHz, DMSO-d_6) δ = 3.74 (br s, 3H, OCH_3), 6.92 (d, *J* = 9.0 Hz, 2H, H-3’’,5’’), 7.15 (s, 1H, CH), 7.51-7.66 (m, 5H, H-2’’,6’’, H-3’’’,5’’’ and H-4’’’), 7.86 (d, *J* = 8.6 Hz, 2H, H-2’,6’), 8.01 (d, *J* = 8.5 Hz, 2H, H-2’’’,6’’’), 8.25 (d, *J* = 8.6 Hz, H-3’,5’), 10.23 (s, 1H, NH), 10.27 (s, 1H, NH) ppm. ^{13}C NMR (75 MHz, DMSO-d_6) δ = 55.2 (OCH_3), 113.7 (C-3’’,5’’), 121.5 (C-2’’,6’’), 123.6 (C-3’,5’), 124.4 (CH), 128.0 (C-2’’’,6’’’), 128.4 (C-3’’’,5’’’), 130.2 (C-2’,6’), 132.0 (C-4’’’), 132.2 (C-1’’), 133.2 (C-1’’’), 134.5 (NH*C*CO), 141.6 (C-1’ or C-4’), 146.4 (C-1’ or C-4’), 155.5 (C-4’’), 163.5 (C*C*ONH), 165.9 (*C*ONHC) ppm. MS *m/z* (ESI %): 418.1 ($[M+H]^+$); HMRS: m/z (ESI) calc. for $C_{23}H_{20}N_3O_5$ 418.1397, found 418.1418.

*2.3. General procedure for the synthesis of Imidazolone derivatives **4a-c***

Anhydrous $ZnCl_2$ (2.5 mmol) was added to the benzamide derivative (0.5 mmol) in toluene (10 mL). The reaction mixture was refluxed for 5-18 h followed by addition of H_2O (25 mL), the pH was adjusted to 3-4 with diluted HCl and the solution extracted with CH_2Cl_2 (3×25 mL). The organic layer was collected, dried with anhydrous Na_2SO_4, and the solvent was evaporated to give a solid residue that was purified by silica gel column chromatography using dichloromethane as eluent.

*2.3.1. (Z)-5-(4-(dimethylamino)benzylidene)-3-(4-methoxyphenyl)-2-phenyl-3,5-dihydro-4H-imidazol-4-one (**4a**)*

The product was isolated as an orange solid (0.112 g, 0.28 mmol, 55 %); R_f 0.46 (CH_2Cl_2). M.p. = 263-264 ºC. ^{1}H NMR (300 MHz, $CDCl_3$) δ = 3.09 (s, 6H, $N(CH_3)_2$), 3.83 (s, 3H, OCH_3), 6.75 (d, *J* = 8.5 Hz, 2H, H-3’,5’), 6.93 (dd, *J* = 8.9 and 1.1 Hz, 2H, H-3’’,5’’), 7.11 (dd, *J* = 8.9 and 1.1 Hz, 2H, H-2’’,6’’), 7.27-7.33 (m, 2H, H-3’’’,5’’’), 7.30 (s, 1H, CH), 7.36-7.42 (m, 1H, H-4’’’), 7.58 (dd, *J* = 8.4 and 1.5 Hz, 2H, H-2’’’,6’’’), 8.23 (d, *J* = 8.5 Hz, 2H, H-2’,6’) ppm. ^{13}C NMR (75 MHz, $CDCl_3$) δ = 40.2 ($N(CH_3)_2$), 55.6 (OCH_3), 111.9 (C-3’,5’), 114.8 (C-3’’,5’’), 122.7 (C-1’), 128.1 (C-1’’), 128.3 (C-3’’’,5’’’), 128.7 (C-2’’,6’’), 129.1 (C-2’’’,6’’’), 129.6 (C-4), 130.7 (C-4’’’), 131.0 (CH), 134.7 (C-1’’’), 134.9 (C-2’,6’), 151.9 (C-

4'), 157.3 (C-2), 159.3 (C-4''), 171.0 (CO) ppm. MS *m/z* (ESI %): 398.4 ($[M+H]^+$); HMRS: m/z (ESI) calc. for $C_{25}H_{24}N_3O_2$ 398.1863, found 398.1887.

*2.3.2. (Z)-5-(4-methoxybenzylidene)-3-(4-methoxyphenyl)-2-phenyl-3,5-dihydro-4H-imidazol-4-one (**4b**)*

The product was isolated as a yellow solid (0.107 g, 0.27 mmol, 54 %); R_f 0.64 (CH_2Cl_2). M.p. = 195-197 ºC. ^{1}H NMR (300 MHz, $CDCl_3$) δ = 3.09 (s, 6H, $N(CH_3)_2$), 3.83 (s, 3H, OCH_3), 6.75 (d, *J* = 8.5 Hz, 2H, H-3',5'), 6.93 (dd, *J* = 8.9 and 1.1 Hz, 2H, H-3'',5''), 7.11 (dd, *J* = 8.9 and 1.1 Hz, 2H, H-2'',6''), 7.27-7.33 (m, 2H, H-3''',5'''), 7.30 (s, 1H, CH), 7.36-7.42 (m, 1H, H-4'''), 7.58 (dd, *J* = 8.4 and 1.5 Hz, 2H, H-2''',6'''), 8.23 (d, *J* = 8.5 Hz, 2H, H-2',6') ppm. ^{13}C NMR (75 MHz, $CDCl_3$) δ = 40.2 ($N(CH_3)_2$), 55.6 (OCH_3), 111.9 (C-3',5'), 114.8 (C-3'',5''), 122.7 (C-1'), 128.1 (C-1''), 128.3 (C-3''',5'''), 128.7 (C-2'',6''), 129.1 (C-2''',6'''), 129.6 (C-4), 130.7 (C-4'''), 131.0 (CH), 134.7 (C-1'''), 134.9 (C-2',6'), 151.9 (C-4'), 157.3 (C-2), 159.3 (C-4''), 171.0 (CO) ppm. MS *m/z* (ESI %): 385.3 ($[M+H]^+$); HMRS: m/z (ESI) calc. for $C_{24}H_{21}N_2O_3$ 385.1547, found 385.1563.

*2.3.3. (Z)-5-(4-nitroxybenzylidene)-3-(4-methoxyphenyl)-2-phenyl-3,5-dihydro-4H-imidazol-4-one (**4c**)*

The product was isolated as a yellow solid (0.092 g, 0.23 mmol, 46 %); R_f 0.73 (CH_2Cl_2). M.p. = 198-200 ºC. ^{1}H NMR (300 MHz, $CDCl_3$) δ = 3.85 (s, 3H, OCH_3), 6.96 (dd, *J* = 8.9 and 2.6 Hz, 2H, H-3'',5''), 7.12 (dd, *J* = 8.9 and 2.6 Hz, 2H, H-2'',6''), 7.28 (s, 1H, CH), 7.34-7.39 (m, 2H, H-3''',5'''), 7.47-7.52 (m, 1H, H-4'''), 7.64 (dd, *J* = 7.2 and 1.5 Hz, 2H, H-2''', H6'''), 8.30 (d, *J* = 8.7 Hz, 2H, H-3',5'), 8.44 (d, *J* = 8.7 Hz, 2H, H-2',6') ppm. ^{13}C NMR (75 MHz, $CDCl_3$) δ = 55.5 (OCH_3), 114.8 (C-3'',5''), 123.8 (C-3',5'), 124.8 (C=*C*-H), 126. 8 (C-1''), 128.2 (C-1'''), 128.4 (C-2'',6'' and C-3''',5'''), 129.4 (C-2''',6'''), 132.0 (C-4'''), 132.8 (C-2',6'), 140.5 (C-4'), 141.1 (C-4), 147.8 (C-1'), 159.6 (C-4''), 163.0 (C-2), 170.6 (CO) ppm. MS *m/z* (ESI %): 400.3 ($[M+H]^+$); HMRS: m/z (ESI) calc. for $C_{23}H_{18}N_3O_4$ 400.1292, found 400.1314.

3. Results and discussion

3.1. Synthesis and characterization

The synthetic route chosen to obtain the fluorophores comprised three steps (Scheme 1). First, the aldehydes **1a-c** were reacted with hippuric acid and sodium acetate in acetic anhydride, following Erlenmeyer azlactone synthesis, and the oxazolones **2a-c** were obtained in 34-47% yields after recrystallization [12]. They were reacted with *p*-anisidine at *ca*. 70 ºC without solvent, to give the ring-opened benzamides **3a-c** in 50-79% yields. Finally, the cyclization of the benzamides in refluxing toluene with anhydrous $ZnCl_2$ afforded the fluorophores **4a-c** in 46-55% yields [13]. All new compounds were fully characterized by ^{1}H and ^{13}C-NMR and HRMS.

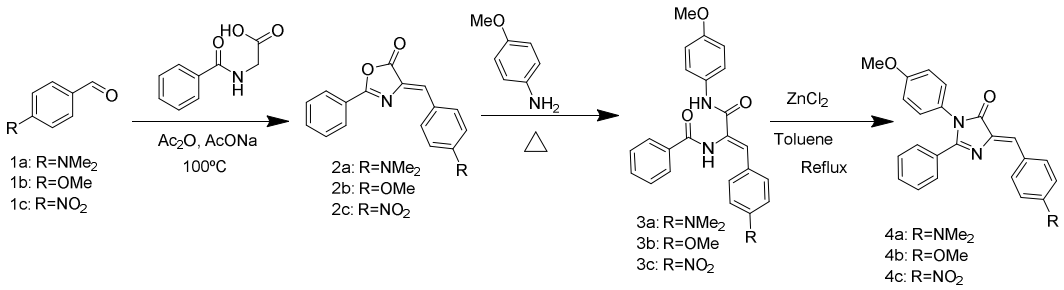

Scheme 1: Synthesis of the chromophores **4a-c**.

3.2. Absorption and emission properties

The absorption and emission properties of the fluorophores **4a-c** were characterized in THF solutions, and the results are summarized in Table 1 and Figure 2. In dilute solution, the fluorophores present a major absorption band at 400-450 nm. As expected [14], the introduction in **4a** of a more electron-donating group, as compared to **4b**, red shifts the absorption and increases the molar extinction coefficient. Likewise, it also red shifts the maximum of emission to 530 nm. The effect of the nitro substituent is more difficult to assess, because compound **4c** presents two emission bands of very low intensities, around 440 and 470 nm. Indeed, fluorophores with nitro substituents tend to present a strong solvatochromism [11i] for both absorption and emission, and double bands emission has been described for fluorophores bearing a nitro substituent [15]. The fluorophores **4a-c** are only weakly emissive in dilute solution, with quantum yields of less than 0.5%. These low quantum yields are expected in solution, because GFP fluorophore analogues are known to relax through the (*Z*-*E*)-isomerisation of the carbon-carbon double bond, making them non-emissive [8b].

Table 1: UV-visible absorption and fluorescence data of compounds **4a-c** ~~in THF~~.

Dye	UV/vis in THF		Fluorescence in THF			Solid state Fluorescence
	λ_{abs} (nm)	ε (M^{-1} cm^{-1})[(a)]	λ_{em} (nm) [(b)]	Stokes' shift (cm^{-1})	φf (%)[(c)]	φf (%)[(d)]
4a	450	51 000	530	3354	< 0.5	1
4b	400	25 000	470	3723	< 0.5	1
4c	410	22 000	440, 470	3982	< 0.1	6

[(a)] ε was determined by linear regression of 4 measurements in the range 10^{-4}M to 10^{-6}M.
[(b)] Excitation at the maximum of absorption.
[(c)] Quantum yields were determined by comparison with fluorescein (quantum yield 0.90 at excitation 470 nm in a solution of NaOH 0.01 M in water) [16].
[(d)] Quantum yields were determined using an integrating sphere.

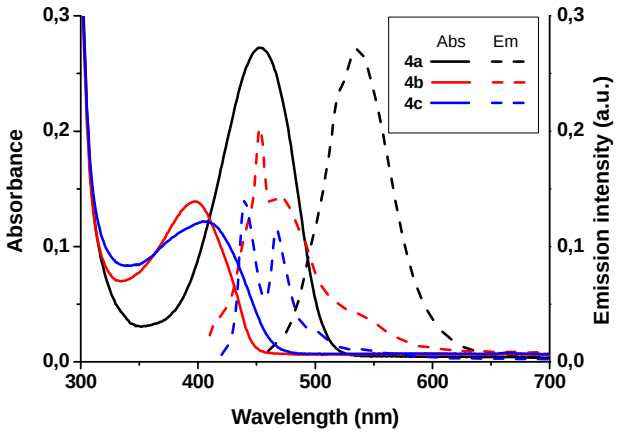

Figure 2. Absorption and emission spectra of fluorophores **4a-c** in THF.

This isomerization can be effectively blocked in the β-barrel of GFP, or when the fluorophore is in the crystalline state. The latter is a particular case of AIEE, when the formation of aggregates or crystals limits internal conversion and forces a dye to emit. In order to assess the AIEE features of the dyes **4a-c**, the emission of their solutions and suspensions in THF-water mixtures was recorded. As **4a** and **4b** present a similar behavior only **4a** is shown here as an example (see Figure 3 and SI). It is almost non-emissive when fully dissolved in THF and when the amount of water is increased up to 60%. When the proportion of water reaches 70% of the mixture, the dye starts to precipitate, and the emission intensity increases by a factor of 100. Because the emission wavelength does not vary, the formation of *J*- or *H*-aggregates can be ruled out [17]. The same observation can be made for **4b**, but not for **4c** which remains almost non-emissive even in the aggregated form, which was expected because water can have a quenching effect for fluorophores bearing a nitro group [11i,18]. These observations were corroborated with the measure of the solid state quantum yields, which are higher than in dilute solution for all three fluorophores.

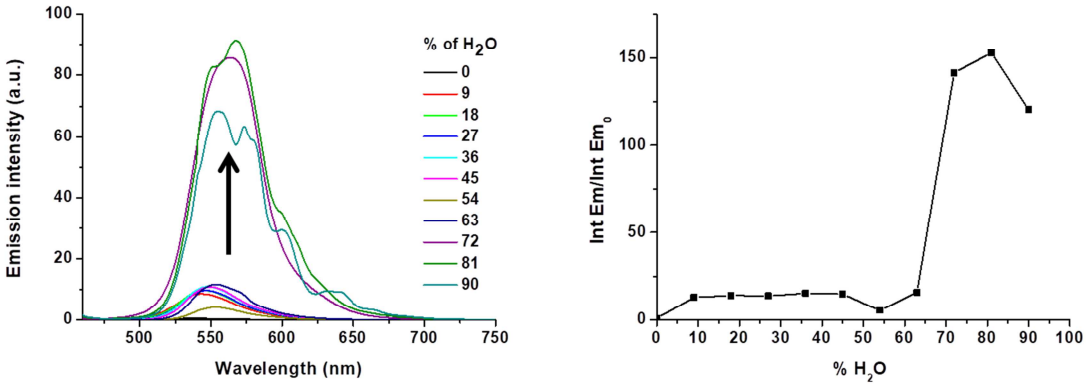

Figure 3. Aggregation-Induced Emission Enhancement observed for compound **4a**. Emission spectra of solutions and suspension of **4a** in THF-water mixtures (left) and relative emission intensity as a function of the water percentage (right).

3.3. Crystal structures

Single crystals suitable for X-ray diffraction were obtained for the fluorophores **4b** and **4c**. All angles and bond lengths are in normal range [19], and the crystal structures confirm the *Z* configuration of the double bond (Figures 4 and 5).
Compound **4b** crystallizes in the triclinic group P-1. One weak intramolecular hydrogen bond C-H···N can be noticed. In the crystal packing, **4b** arranges into columns held together via weak intermolecular hydrogen bonds and Van der Waals interactions (Figure 4).

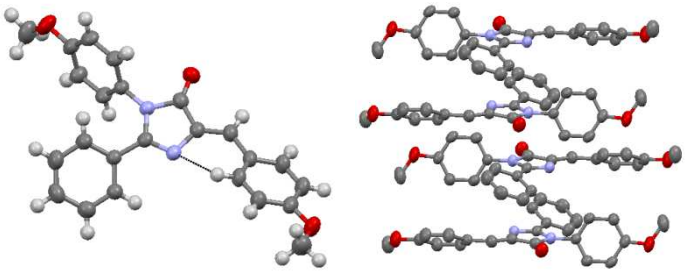

Figure 4. Molecular structure of compound **4b** (left) and columnar arrangement (right, hydrogen atoms not shown, for clarity). Thermal ellipsoids are shown at the 50% probability level, hydrogen atoms are depicted with an arbitrary radius (0.30Å), and the hydrogen bond in dashed black line. C, grey; O, red; N, blue; H, white.

Compound **4c** crystallizes with one molecule of chloroform in the triclinic group P-1. The chloroform molecule forms a hydrogen bond with the amide oxygen, and a weak intramolecular hydrogen bond is present between an aromatic C-H and a nitrogen atom. In the crystal packing, the fluorophores arrange into dimers, held together via weak hydrogen bonds and Van der Waals interactions, and the dimers further arrange into columns (figure 5).

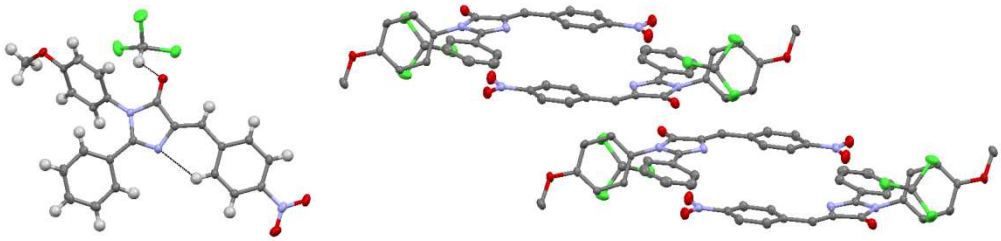

Figure 5. Molecular structure of compound **4c** and chloroform (left) and columnar arrangement (right, hydrogens atoms not shown, for clarity). Thermal ellipsoids are shown at the 50% probability level, hydrogen atoms are depicted with an arbitrary radius (0.30Å). C, grey; O, red; N, blue; H, white; Cl, green.

The crystal structures reveal that no strong intermolecular interactions are present, and the fluorophores do not form *J*- or *H*-aggregates. This is accord with the fact that the emission wavelengths in the solution and solid state are the same. Moreover, the crystal packing

efficiently blocks the *Z*/*E* isomerisation of the double bond, turning the fluorophore more emissive in the crystalline state than in solution.

4. Conclusion

Three analogues of the GFP fluorophore were synthesized in moderate yields using a straightforward strategy. In solution, they display fluorescence quantum yields of less than 0.5% and moderate Stokes' shifts, between 70 and 80 nm. Their emission intensity increases dramatically in the solid state, thanks to the restriction of their intramolecular motion. The crystal structures confirmed the (*Z*)-conformation of the double bond, which is blocked in the solid state but not in solution, confirming the (*Z*/*E*)-isomerization is the main relaxation pathway in solution. The introduction of more electron-donating substituents on the aromatic ring connected to the carbon-carbon double bond red shifts the absorption and emission. In contrast, the anisole ring is almost perpendicular to the imidazolidinone, meaning that it does not participate in the conjugation of the aromatic system of the dye, and could be modified in order to tune its physical-chemical properties without modifying its photophysics.

Acknowledgment

Thanks are due to University of Aveiro, FCT/MEC for the financial support to the QOPNA research Unit (FCT UID/QUI/00062/2019) and also to the Portuguese NMR Network. This work was developed within the scope of the project CICECO-Aveiro Institute of Materials, FCT Ref. UID/CTM/ 50011/2019, financed by national funds through the FCT/MCTES. S. Guieu acknowledges the fundings from national funds (OE), through FCT – Fundação para a Ciência e a Tecnologia , I.P., in the scope of the framework contract foreseen in the numbers 4, 5 and 6 of the article 23, of the Decree-Law 57/2016, of August 29, changed by Law 57/2017, of July 19, and from the Integrated Programme of SR&TD “pAGE – Protein aggregation Across the Lifespan” (reference CENTRO-01-0145-FEDER-000003). C.I.C. Esteves acknowledges the 016385-PAC NETDIAMOND project (POCI-01-0145-FEDER-016385) for her Post-Doctoral grant (BPD/UI50/7664/2017). Professor Rute AS Ferreira (phantom-g, CICECO, Department of Physics, University of Aveiro) is acknowledged for the solid state quantum yield measurements.

Appendix A. Supplementary data.

Experimental procedures, compound characterization data and NMR spectra of the new compounds. CCDC-1958327-1958328 contain the supplementary crystallographic data for this paper. These data can be obtained free of charge at www.ccdc.cam.ac.uk/conts/retrieving.html (or from the Cambridge Crystallographic Data Centre, 12, Union Road, Cambridge CB2 1EZ, UK. Fax: C44 1223 336 033. E-mail: deposit@ccdc.cam.ac.uk).

References

[1] Stepanenko OV, Verkhusha VV, Kuznetsova IM, Uversky VN, Turoverov KK. Fluorescent Proteins as Biomarkers and Biosensors: Throwing Color Lights on Molecular and Cellular Processes. Curr Protein Pept Sci 2009;9:338-69;

[2] Follenius-Wund A, Bourotte M, Schmitt M, Iyice F, Lami H, Bourguignon J-J, Haiech J, Pigault C. Fluorescent Derivatives of the GFP Chromophore Give a New Insight into the GFP Fluorescence Process. Biophys J 2003;85:1839-50, DOI: 10.1016/S0006-3495(03)74612-8;

[3] Wiedenmann J, Oswald F, Nienhaus GU. Fluorescent Proteins for Live Cell Imaging: Opportunities, Limitations, and Challenges. IUBMB Life 2009;61:1029-42, DOI: 10.1002/iub.256;

[4] (a) Walker CL, Lukyanov KA, Yampolsky IV, Mishin AS, Bommarius AS, Duraj-Thatte AM, Azizi B, Tolbert LM, Solntsev KM Fluorescence imaging using synthetic GFP chromophores. Curr Opin Chem Biol 2015;27:64-74, DOI: 10.1016/j.cbpa.2015.06.002;
(b) Deng H, Zhang Z, Zhao Y, Yu C, Gong L, Yan D, Zhu X. Self-restricted oxazolone GFP chromophore for construction of reaction-based fluorescent probe toward dopamine. Mater Today Chem 2017;3:73-81, DOI: 10.1021/acs.jpclett.6b01251;

[5] Shaner NC, Patterson GH, Davidson MW. Advances in fluorescent protein technology. J Cell Sci 2007;120:4247-60; DOI: 10.1242/jcs.005801;

[6] Tolbert LM, Baldridge A, Kowalik J, Solntsev KM. Collapse and Recovery of Green Fluorescent Protein Chromophore Emission through Topological Effects. Acc Chem Res 2012;45:171-81, DOI: 10.1021/ar2000925;

[7] Frizler M, Yampolsky IV, Baranov MS, Stirnberg M, Gütschow M. Chemical introduction of the green fluorescence: imaging of cysteine cathepsins by an irreversibly locked GFP fluorophore. Org Biomol Chem 2013;11:5913-21, DOI: 10.1039/C3OB41341A;

[8] (a) Chatterjee S, Karuso P. An efficient and concise method to synthesize locked GFP chromophore analogues. Tetrahedron Lett 2016;57:5197-200, DOI: 10.1016/j.tetlet.2016.10.021;
(b) Ikejiri M, Kojima H, Fugono Y, Fujisaka A, Chihara Y, Miyashita K. Synthesis and properties of geometrical 4-diarylmethylene analogs of the green fluorescent protein chromophore. Org Biomol Chem 2018;16:2397-401, DOI: 10.1039/C8OB00208H;
(c) Wu L, Burgess K. Syntheses of Highly Fluorescent GFP-Chromophore Analogues. J Am Chem Soc 2008;130:4089-96; DOI: 10.1021/ja710388h;
(d) Mirajkar AL, Mittapelli LL, Nawale GN, Gore KR. Synthetic green fluorescent protein (GFP) chromophore analog for rapid, selective and sensitive detection of cyanide in water and in living cells. Sens Act B Chem 2018;265:257-63, DOI: 10.1016/j.snb.2018.03.068;

[9] (a) Wu L, Burgess K. Syntheses of Highly Fluorescent GFP-Chromophore Analogues. J Am Chem Soc 2008;130:4089-96, DOI: 10.1021/ja710388h;
(b) Conyard J, Heisler IA, Chan Y, Page PCB, Meech SR, Blancafort L. A new twist in the photophysics of the GFP chromophore: a volume-conserving molecular torsion couple. Chem Sci 2018;9:1803–12; DOI: 10.1039/C7SC04091A;

[10] (a) Dong J, Solntsev KM, Tolbert LM. Activation and Tuning of Green Fluorescent Protein Chromophore Emission by Alkyl Substituent-Mediated Crystal Packing. J Am Chem Soc 2009;131:662-70; DOI: 10.1021/ja806962e;

(b) Ge S, Deng H, Su Y, Zhu X. Emission enhancement of GFP chromophore in aggregated state *via* combination of self-restricted effect and supramolecular host-guest complexation. RSC Adv 2017;7:17980-7, DOI: 10.1039/C7RA00974G;

(c) Liu Y, Wolstenholme CH, Carter GC, Liu H, Hu H, Grainger LS, Miao K, Fares M, Hoelzel CA, Yennawar HP, Ning G, Du M, Bai L, Li X, Zhang X. Modulation of fluorescent protein chromophores to detect protein aggregation with turn-on fluorescence. J Am Chem Soc 2018;24:7381-7384; DOI: 10.1021/jacs.8b02176;

[11] (a) Guieu S, Cardona F, Rocha J, Silva AMS. Tunable Color of Aggregation-Induced Emission Enhancement in a Family of Hydrogen-Bonded Azines and Schiff Bases. Chem Eur J 2018;24:17262-7; DOI: 10.1002/chem.201802581;

(b) Guieu S, Rocha J, Silva AMS. Crystallization-induced light-emission enhancement of diphenylmethane derivatives. Tetrahedron 2013;69:9329-34; DOI: 10.1016/j.tet.2013.07.107;

(c) Vaz PAAM, Rocha J, Silva AMS, Guieu S. Aggregation-induced emission enhancement in halochalcones. New J Chem 2016;40:8198-201; DOI: 10.1039/C6NJ01387B;

(d) Vaz PAAM, Rocha J, Silva AMS, Guieu S. Aggregation-induced emission enhancement of chiral boranils. New J Chem 2018;42:18166-71; DOI: 10.1039/C8NJ03228A;

(e) Zhang X, Chi Z, Xu B, Chen C, Zhou X, Zhang Y, Liu S, Xu J. End-group effects of piezofluorochromic aggregation-induced enhanced emission compounds containing distyrylanthracene. J Mater Chem 2012;22:18505-18513; DOI: 10.1039/C2JM33140C;

(f) Zhang X, Chi Z, Li H, Xu B, Li X, Zhou W, Liu S, Zhang Y, Xu J. Piezofluorochromism of an Aggregation□Induced Emission Compound Derived from Tetraphenylethylene. Chem-Asian J 2011;6: 808-811. DOI: 10.1002/asia.201000802;

(g) Mei J, Leung NLC, Kwok RTK, Lam JWY, Tang BZ. Aggregation-induced emission: together we shine, united we soar! Chem Rev 2015;21:11718-11940. DOI: 10.1021/acs.chemrev.5b00263;

(h) Yang L, Fang W, Ye Y, Wang Z, Hua Q, Tang BZ. Redox-responsive fluorescent AIE bioconjugate with aggregation enhanced retention features for targeted imaging reinforcement and selective suppression of cancer cells. Mater Chem Front 2019;3:1335-1340; DOI: 10.1039/C9QM00216B;

(i) Baig MZK, Prusti B, Roy D, Sahu PK, Sarkar M, Sharma A, Chakravarty M. Weak donor-/strong acceptor-linked anthracenyl π□conjugates as solvato(fluoro)chromophore and AEEgens: Contrast between nitro and cyano functionality. ACS Omega 2018;3:9114-9125; DOI: 10.1021/acsomega.8b01258;

[12] Roiban G-D, Soler T, Grosu I, Cativiela C, Urriolabeitia EP. Unsaturated 4,4'-bis-[5(4H)-oxazolones]: Synthesis and evaluation of their ortho-palladation through C–H bond activation. Inorg Chim Acta 2011;368:247-51; DOI: 10.1016/j.ica.2010.12.054;

[13] Rajbongshi BK, Ramanathan G. Dominant π···π interaction in the self assemblies of 4-benzylidene imidazolin-5-one analogues. J Chem Sci 2009;121:973-82; DOI: 10.1007/s12039-009-0126-4;

[14] Guieu S, Pinto J, Silva VLM, Rocha J, Silva AMS. Synthesis, post-modification and fluorescence properties of boron-diketonate complexes. Eur J Org Chem 2015;3423-26; DOI: 10.1002/ejoc.201500318;

[15] Esnal I, Bañuelos J, Arbeloa IL, Costela A, Garcia-Moreno I, Garzón M, Agarrabeitia AR, Ortiz MJ. Nitro and amino BODIPYS: crucial substituents to modulate their photonic behavior. RSC Adv 2013;3:1547-1556; DOI: 10.1039/c2ra22916a;

[16] Crosby GA, Demas JN. Measurement of photoluminescence quantum yields. Review. Phys Chem 1971;75:991-1024; DOI:10.1021/j100678a001;

[17] Würthner F, Kaiser TE, Saha-Möller CR. J-aggregates: from serendipitous discovery to supramolecular engineering of functional dye materials. Angew Chem Int Ed 2011;50:3376-410; DOI: 10.1002/anie.201002307;

[18] (a) Esteves CIC, Raposo MMM, Costa SPG. Non-canonical amino acids bearing thiophene and bithiophene: synthesis by an Ugi multicomponent reaction and studies on ion recognition ability. Amino Acids 2017;49:921-30; DOI: 10.1007/s00726-017-2392-7;
(b) Esteves CIC, Raposo MMM, Costa SPG. Novel highly emissive non-proteinogenic amino acids: synthesis of 1,3,4-thiadiazolyl asparagines and evaluation as fluorimetric chemosensors for biologically relevant transition metal cations. Amino Acids 2011;40:1065-75; DOI: 10.1007/s00726-010-0730-0;

[19] Allen FH, Kennard O, Watson DG, Brammer L, Orpen AG, Taylor RJ. Tables of bond lengths determined by ***X***-ray and neutron diffraction. Part 1. Bond lengths in organic compounds. J. Chem Soc Perkin Trans 1987;2:1-19. DOI: 10.1039/P298700000S1.

[20] Khadse SC, Chatpalliwar VA. Synthesis of benzamides by microwave assisted ring opening of less reactive dimethylaminobenzylidene oxazolone. Arab J Chem 2017;10:S859-S863. DOI: 10.1016/j.arabjc.2012.12.020

Highlights

A new synthesis of analogues of the Green Fluorescent Protein fluorophore is presented.

They are almost non emissive in solution.

Their emission intensity increases up to a hundred times upon crystallization.

Changing the substituents tunes their absorption and emission spectra.

Declaration of interests

☒ The authors declare that they have no known competing financial interests or personal relationships that could have appeared to influence the work reported in this paper.

☐The authors declare the following financial interests/personal relationships which may be considered as potential competing interests: